geoconvention
Calgary • Canada • May 7-11 2018

Prestack P-P Azimuthal Amplitudes in the Washout 3D full azimuth full offset survey

Heloise B. Lynn, Lynn Inc., and Mike Perz, TGS Calgary

Summary

Azimuthal prestack amplitude analysis for the Top/Viking was performed in order to evaluate this high S/N shale-sandstone reflector. Both Standard Ruger (1997; fixed intercept) and Nonstandard AVOaz analysis (floating intercept) were performed. Both methods showed the artifacts caused by large holes of skipped shots and/or skipped receiver locations. Areas of uniform shooting were inspected to compare the Standard Ruger and the Nonstandard AVOaz results. The Biso (AVO gradient common to all azimuths) was similar in both methods. Some bins showed the azimuthal variation on the near-angle amplitudes to be minimal, and so the two methods gave similar results. In other bins in the survey, the azimuthal variation of the near-angle amplitudes was significant, and so only the Nonstandard AVOaz (floating intercept) gave results that match the field data. Using the floating intercept AVOaz method, we see that the estimated azimuth of most negative AVO gradient exhibits a very strong correspondence to the estimated azimuth of the highest amplitude intercept (near-angle amplitude), as expected, and is interpreted as the fracture parallel direction.

Introduction

P-P prestack azimuthal amplitudes in field data have been studied since the mid-1990s (Lynn et al., 1995). Recent publications (Lynn et al, 2014; Lynn 2014a,b,c; 2015, 2016) have shown that for a given CIG bin, the higher effective porosity sensed azimuth (fracture perpendicular) has dimmer Near Angle amplitudes and less negative (more positive) AVO gradient. The lower effective porosity sensed azimuth (fracture-parallel) has the most bright mathematical intercepts (Near Angle amplitudes) and the most negative AVO gradients for the given CIG bin. Lynn uses the non-standard AVOaz method, where the intercept is allowed to float by azimuth, in the calculation of the AVO gradient (by azimuth). This preserves the information on the near angle amplitudes. The azimuth of most bright mathematical Intercept (near angle amplitude) tracks the azimuth of most negative AVO gradient. A crossplot of the azimuthal (Near-angle amplitudes, AVO gradients) for the CIG presents a straight line, and demonstrates effective porosity sensed changing by azimuth (Lynn and Goodway, 2018). In these Lynn field dataset papers, the reflection is from a low impedance shale over a high impedance carbonate, with the higher fracture density expected in the carbonate. The carbonate flows oil with sufficient fracture density.

Azimuthal near angle amplitudes were also reported by Pan et al. (2017) who published 3D azimuthal P-P field data. They showed, also with modeling and rock physics equations, that processing for and analysis of the azimuthal elastic impedance for fluid indicators can reveal the presence of pay in their fractured carbonate reservoir. The azimuthal AVO gradient gives the estimate of fracture density for each bin [the azimuthal S-impedance] ; the azimuthal near-angle amplitudes give the azimuthal P impedance which is interpreted to indicate either gas or liquid. Obviously, the fracture model is one set of vertical aligned fractures.

Other recent publications (Wang et al., 2015, Deng et al. 2012, Deng et al 2013, Ekanem et al., 2015, Luo et al., 2017) have demonstrated that azimuthal variations in Q may exist, be mapped, modeled, and tied to well data and production using 3D P-P and P-S field data, when one set of vertical aligned meso-fractures are present. An azimuth-dependent wave-induced fluid-flow mechanism between pore and mesoscopic fractures is cited for the azimuthal Q. The wave traveling in the fracture-perpendicular propagation causes greater fluid movement between pore-crack-pore, but fracture-parallel wave propagation causes less.

Theory and Method

The two AVOaz methods, Ruger (1997; and Ruger and Tsvankin, 1997) and Nonstandard AVOaz, give different results when the azimuthal variation of the near angles is significant. The two methods give similar results when the far angle azimuthal amplitudes cause the AVO gradient change by azimuth (that is, the near-angles have little azimuthal variation). One area in the Washout survey was examined where the two methods gave different results. The gathers were examined: the Nonstandard AVOaz (floating intercept) analysis faithfully recorded what the gathers showed; by contrast, the Standard Ruger result was not present in the field data. This data examination clearly shows that when the mathematical intercept is allowed to float by azimuth, then these near-angle azimuthal amplitudes can be reliably captured. The azimuthal variation of the near angle amplitudes appears to be signal, although further work, including a comprehensive visualization of both final-processed and raw data in various domains, is ongoing in order to rule out the possibility that such variation might be due to azimuthal variations in coherent noise (with preliminary analysis suggesting that noise is not creating the variation)

We are still investigating the relative contribution of the following mechanisms: a) VP varies by azimuth, even at small angles of incidence, due to the shear modulus varying by azimuth (shear-wave splitting) and effective porosity sensed changing by azimuth; b) azimuthally variable strength in the diffractions may affect the coherent reflection signal; c) azimuthal Q due to fluid-flow -squirt differences by azimuth in naturally fractured porous media is affecting the near-angle amplitudes d) azimuth-dependent optical diffraction grating reflection effects due to one set of vertical aligned fractures .

In the Washout survey, examination of the relationship of the azimuth of the most positive Mathematical Intercept (floating intercept analysis) and the azimuth of the most negative AVO gradient showed that these azimuths matched within 21 degrees of each other for 3/4ths of the bins of the survey. Furthermore, these two azimuths matched within 10 degrees of each other for half the bins of the survey. Thus, considering the ~150,000 bins of the survey, **75,000 bins had matching azimuths within 10 degrees of each other**. This similarity in azimuths is to be expected, as per the following argument.

Hilterman (2018) shows the effect of porosity and pore fluid upon the Top/Sandstone reflector when its Normal Incidence (mathematical intercept) and its Slope (AVO gradient) are analyzed in the azimuth-blind P-P reflection (Figure 1).

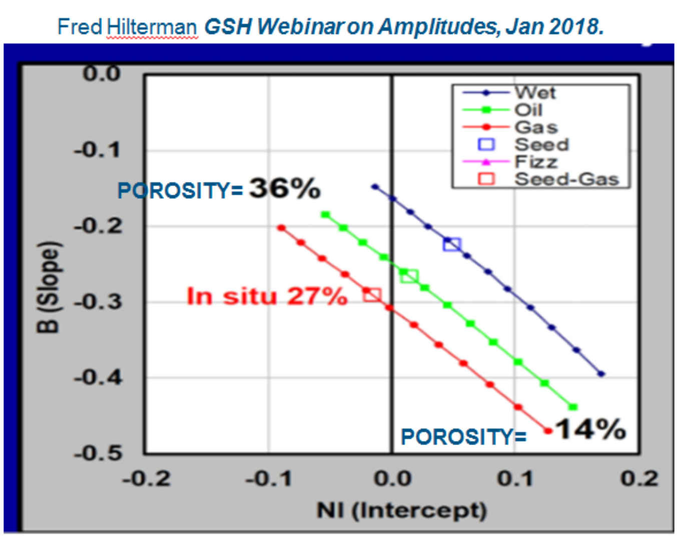

Figure 1. When lithology contrast (here, low impedance shale over high impedance sandstone) and pore fluid are held constant, the effect of increasing porosity is to decrease the Normal Incidence (Intercept) amplitude and cause the AVO gradient (slope) to become less negative (that is, to become more positive).

Hilterman presents straight lines on the crossplot, with brightest Mathematical Intercept linked to most negative AVO gradient in the case of ***low*** porosity; the dimmest Intercept is linked to a flatter (more positive) AVO gradient in the case of ***high*** porosity. This result provides a heuristic framework for interpreting azimuth-dependent AVO gradients (and mathematical intercepts, or Near Angle Amplitudes).

We have adapted his figure by inserting labels, “fracture-perpendicular” and “fracture-parallel” to indicate the change in the effective porosity sensed by the wave. The fracture perpendicular direction senses Matrix+Fracture porosity; the fracture parallel direction senses Matrix porosity alone, as shown in Figure 2.

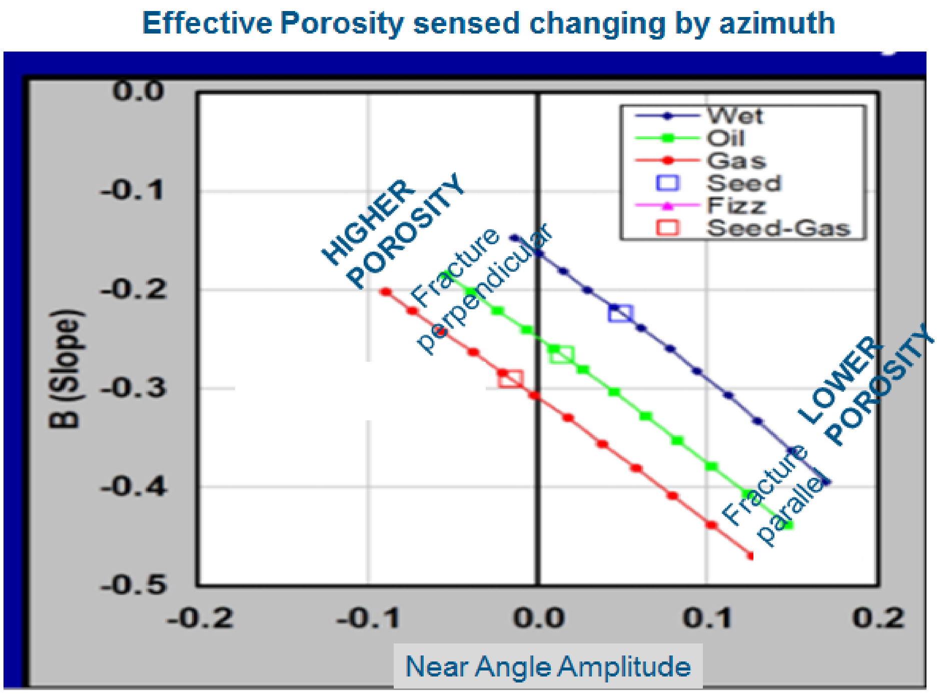

Figure 2. The crossplot of Near Angle Amplitude versus AVO gradient, expanded into the azimuthal world. We added the fracture-parallel and fracture-perpendicular labels. The model is a low impedance shale over a high impedance sandstone. Lithology is held fixed; pore fluid is held fixed. The higher fracture density is in the sandstone. As azimuth changes from fracture parallel to fracture perpendicular, the Near Angle amplitude steadily decreases and the AVO gradient steadily becomes less negative. A given line (for fixed pore fluid) would display, for one CIG bin, the pair of values of the azimuth-dependent AVO gradient and the azimuth-dependent Near-Angle Amplitude (“mathematical Intercept”), for as many azimuths as were processed for, that is, at least six azimuths,   for the given mapped reflector.

This behavior will be shown for the P-P Viking Sandstone of the Washout 3D survey.

Both AVOaz methods showed the artifacts caused by large zones of skipped shots and/or skipped receiver locations. This survey used orthogonal shooting, E-W source lines, N-S receiver lines. “A large zone” here means 2 or 3 source lines not present, for ~2 or 3 receiver lines’ width. Areas of uniform shooting were inspected to compare the Standard Ruger and the Nonstandard AVOaz results. The Biso (AVO gradient common to all azimuths) was similar in both methods. Two different types of AVOaz signatures are observed: those with minimal near-angle amplitude variations, but others with large near-angle amplitude variations. Proper interpretation must attempt to tie each different type back to a known geologic situation, using independent support data (wireline logs, production, VSP, borehole image logs, cores, etc.). Lynn speculates that stress-aligned micro-fractures provide the former AVOaz signature, while macro-fractures that flow fluids provide the latter signature. Lynn and Perz hope that more geophysicists will more carefully scrutinize their AVOaz data and publish calibrated field studies, since distinguishing between these two situations has significant economic consequences.

Conclusions

Large zones of skipped shots and receivers in acquisition leave holes that 5D interpolation can't fill in, and so artifacts in AVOaz are noticed, for both methods. In areas of uniform shooting, the fixed-intercept and the floating-intercept AVOaz methods' results were compared. Where the azimuthal variation of the near angle amplitudes is minimal, then both methods give similar results. In other bins, the near angle amplitudes show significant azimuthal amplitude variation: in these locales, only the floating intercept AVOaz method produces results that match the field data.

Acknowledgements

Bill Shea, Sharp Reflections, granted access to PS PRO Azimuthal, the interpretation platform that enabled this study (Standard Ruger and Nonstandard AVOaz). Ryan Lau, Sharp Reflections, provided the analysis. Bill Goodway has provided persuasive arguments as to why the near angle amplitudes can vary by azimuth (Lynn and Goodway, 2018).

References

Deng, Jixin, Shouli Qu, Shixing Wang, Shengwang Zhu, and Xuben Wnag, 2012, P wave attenuation and dispersion in a porous medium permeated by aligned fractures – a new poroelastic approach, J. Geophys. Eng., 9, No. 2.

Deng, Jixin, Shangxu Wnag, Gengyang Tang, Jianguo Zhao, and Xiangyang Li, 2013,, The influence of mesoscopic flow on the P-wave attenuation and dispersion in a porous media permeated by aligned fractures, Stud. Geophys. Geod., 57, 48-506.

Ekanem, A. M., X.Y. Li, M. Chapman, and I.G. Main, 2015, Seismic attenuation in fracture porous media: insights from a hybrid numerical and analytical model, J. Geophys Eng. 12, No. 2, 210.

Lynn, H.B., R. Bates, M. Layman, M. Jones, 1995, Natural fracture characterization using P-wave reflection seismic data, VSP, borehole imaging logs and the in-situ stress field determination, SPE 29595, SPE Symposium, Denver, CO 20-22 March 1995.

Lynn, H.B., and Goodway, Bill, 2018, Effective porosity sensed changing by azimuth: a linear crossplot of azimuthal P-P (Near Angle Amplitudes, AVO gradients): , 2018 SEG Annual Meeting Expanded Abstract. (submitted)

Lynn, H.B., W. Lynn, J. Obilo, V. Agarwall, 2014, Azimuthal prestack depth migration for in-situ stress evaluation, in a fractured carbonate oil reservoir: predrill prediction of Instantaneous Shut-In Pressure gradients.

Lynn, H.B., 2016, Comparisons of azimuth-blind P-P amplitude variation with angle (AVA) to azimuth-dependent AVA at calibration points of known fracture azimuth and fracture density, SEG Exp. Abs.

Lynn, H.B., 2015, Azimuthal 3D seismic data, ISIP's, and micro-seismic data evaluated for unconventional completions in a fractured reservoir, SEG Exp. Abs.

Lynn, H.B., 2014a, Fracture densities and fracture azimuths evident in the azimuthal amplitudes from the top of a fractured carbonate oil reservoir.

Lynn, H.B., 2014b, Field evidence of orthorhombic media: changes in the P-P bright azimuth with angle of incidence.

Lynn, H.B.., 2014c, Azimuthal anisotropy: distinguishing between unequal horizontal stress and vertical aligned macro-fractures, as demonstrated in thirty years of field data analysis.

Luo, Cong, Xiangyang Li, and Guangtan Huang, 2017, Application of oil-water discrimination technology in fractured reservoirs using the differences between fast and slow shear-waves, **J. Geophys. Eng. 14,** 723-738.

Pan, X., G. Zhang, X. Yin, 2017, Azimuthally anisotropic elastic impedance inversion for fluid indicator driven by rock physics, Geophysics., v. 82, C211-C227.

Ruger, A. 1997, P-wave reflection coefficients for transversely isotropic models with vertical and horizontal axis of symmetry, Geophysics, **62**, 713-722.

Ruger, A. and I. Tsvankin, 1997, Using AVO for fracture detection: Analytic basis and practical solutions, The Leading Edge, 1429-1434.

Wang, Yaojun, Shuangquan Chen, and Xiang-Yang Li, 2015, Anisotropic characteristics of mesoscale fractures and applications to wide azimuth 3D P-wave seismic data, J. Geophys. Eng. 12, 448-464.